IOSR Journal of Applied Physics (IOSR-JAP)
e-ISSN: 2278-4861.Volume 5, Issue 3 (Nov. - Dec. 2013), PP 64-68
www.iosrjournals.org

Structural, Electrical and Magnetotransport properties of $La_{0.7}Ca_{0.2}Sr_{0.1}MnO_3$ by self propagating high temperature synthesis.

P. P. Jagtap[1], Y. A. Chaudhari[2], E. M. Abuassaj[3], P.B. Patil[3] and S. T. Bendre[3,*]

[1]*Department of Physics, P.S.G.V.P.M's Arts, Science and Commerce College, Shahada-425409, India*
[2]*Department of Engineering Sciences and Humanities, SRTTC-FOE, Kamshet, Pune-410405, India*
[3]*Department of physics, North Maharashtra University, Jalgaon-425401, India*

Abstract: *The sample of manganite perovskite oxide $La_{0.7}Ca_{0.2}Sr_{0.1}MnO_3$ has been prepared by solution combustion synthesis. The synthesized sample has been pelletized and further sintered at 800^0C for 8 hours. The XRD pattern reveals that the samples are of single phase nature with orthorhombic structure and the diffraction patterns can be indexed with the pbnm space groups. The crystallite sizes calculated from broadening of XRD peaks using Scherrer's formula were about 18 nm. Resistivity measurements were performed in the temperature range 2K under 3, 5, 10 and 14 T field using PPMS. Magnetoresistance shows a shift in metal-insulator transition temperature from ~213 K at zero field to ~250 K at 14T. MR value decreases as the temperature increases and at 300 K maximum value of MR is found to be ~ 22% for an applied field of 14 T. MR of ~ 28% is observed at 230 K. MR of ~ 35% is observed at 150 K in an applied field of 14 T and MR has negative sign.*

Keywords: *Manganites, Perovskite, Magnetoresistance, Magnetotransport and Combustion Synthesis.*

I. Introduction

Magnetoresistance (MR) has been reported for a variety of systems, such as metallic multilayers, granular inter metallic alloys and manganite perovskite oxides [1-2]. The observation of MR in the hole-doped perovskite manganites of the general formula $RE_{1-x}A_xMnO_3$ (RE = rare earth ion, A = divalent alkaline earth metal ion) has driven considerable interest in the study of these compounds owing to the remarkable magneto transport phenomena and the potential technological applications to new devices such as magnetoresistive read heads, magnetic sensors and magnetic random access memory (MRAM) [3-6].

Perovskite structured lanthanum manganites display strong ferromagnetism and metallic conductivity when trivalent La^{3+} ions are partially substituted for divalent ions like Ca, Ba, Sr etc [7]. The substitution of divalent ions for La^{3+} creates Mn^{3+} to Mn^{4+} mixed valence state resulting mobile charge carriers and canting of Mn spins [8, 9]. The double exchange (DE) interaction of Mn^{3+} and Mn^{4+} pairs, along with Jahn Teller effect lead to the appearance of the so called Magneto resistance (MR) in such systems [10]. It is believed that the DE interaction between Mn^{4+} and Mn^{3+} ion pairs is responsible for the metallic character and ferromagnetic (FM) properties in these manganese oxides. Fast hopping of the d-electrons between the two oxidation states of Mn produces metallic behaviour as the material becomes ferromagnetic giving rise to an insulator-metal (I-M) transition at temperature slightly below the ferromagnetic transition temperature [11, 12].

There are many techniques for the preparation of perovskite based rare earth manganites, which include solid state reaction, sol-gel, citrate-gel, co-precipitation, hydrothermal, microwave techniques etc [13-15]. A majority of work available on the synthesis of manganite perovskite oxides is generally based on high temperature ceramic method.

In this work, our principal motivation was to study electronic transport including magnetoresistance in nanostructured samples of the perovskite based rare earth manganites. These oxides have attracted wide attention as Magnetoresistance (MR) in the last decade [16, 17]. In this work we have investigated a simple and novel method of synthesizing nanocrystalline calcium and strontium substituted lanthanum manganites by solution combustion method using a fuel and oxidizers. It is an important powder processing technique generally used to prepare oxide ceramics [18]. It involves several advantages like fast heating rates, short reaction time, besides producing foamy, homogeneous and high surface area of nanocrystalline products [19].

II. Experimental

2.1 Chemicals:

The chemicals used for the synthesis of $La_{0.}7Ca_{0.2}Sr_{0.1}MnO_3$ using solution combustion synthesis are Lanthanum oxide (99.9%, SRL), Calcium Carbonate (99.9%, LOBA Chemie), Strontium carbonate (99.9%,

LOBA Chemie), Nitric acid (69.72%, LOBA Chemie), Manganese acetate tetrahydrate (99.5%, s.d. fine-chem Ltd.).

2.2 Synthesis of $La_{0.7}Ca_{0.2}Sr_{0.1}MnO_3$ by solution combustion synthesis:

Lanthanum oxide, Calcium Carbonate and Strontium carbonate were separately dissolved in dilute nitric acid to make corresponding nitrates at a molar ratio of lanthanum: calcium and strontium equal to 7:3. To these solutions, an aqueous solution of manganese acetate was added so that the nitrate and acetate (oxidant and fuel) forms a stoichiometric mixture for combustion reaction to occur. The stoichiometry of the fuel and oxidant was calculated based on the total oxidizing and reducing valencies of the oxidizer (O) and the fuel (F), which serve as numerical coefficients so that the equivalence ratio (O/F) becomes unity and heat released is maximum. This solution was then put in a borosil dish and heated with Bunsen burner at about 80^0C to evaporate water until a viscous gel was formed. The water content in the redox mixture appears to influence the phase formation and the properties of the products. A rapid heating result in incomplete evaporation of residual water in the redox mixture at the time of ignition and a viscous gel is obtained. After the gel formation, the dish is rapidly heated by a Bunsen burner. It was found that the ignition commenced at a temperature of 200^0C and a reddish hot region is developed around the reaction area with the release of abundant fumes. At high temperature, the metal nitrates decompose to metal oxides and oxides of nitrogen acts as oxidizer for further combustion that leads to a voluminous foamy combustion residue in less than 2 minutes. The whole process is spectacular and the flame temperature is ~1500^0C. The end product (i.e. foam) obtained in this process is a swelled black powder of LCSMO.

Then the as-formed powder, which is free from any carbon residue was grinded in an agate mortar with pestle by adding acetone in a mixture, until a homogeneous mixture is obtained. Then 3-4 drops of poly vinyl alcohol (PVA), which acts as a binder is added to the powder. Then this powder was crushed and uniaxially pressed into compacts using stainless steel die-punch and hydraulic press by compressing it at 5 tons/cm^2 for a minute to form a pellet. The pellets obtained are of the size of 16 mm diameter and thickness of ~2-5 mm.

The pellets are finally sintered at 800^0C for 8 hours. The sintering process provides the energy to encourage the individual powder particles to bond together to remove the porosity present from the compaction stages. These pellets (i.e. final material) are further used for the characterizations.

III. Results And Discussion

3.1 X-Ray diffraction:

Fig. 5.1 shows XRD spectrum of $La_{0.7}Ca_{0.2}Sr_{0.1}MnO_3$ sample. It reveals pure single phase nature. The diffraction peaks of $La_{0.7}Ca_{0.2}Sr_{0.1}MnO_3$ are sharp and crystallize in orthorhombic structure having pbnm space group. The lattice parameters were obtained as a=5.48 A^0, b=7.77 A^0 and c=5.546 A^0 and cell volume as V = 232.3 $(A^0)^3$. The broadness of XRD peaks indicates the nanocrystalline nature of the combustion derived products. Crystallite sizes were calculated from the broadening of XRD peaks using the Scherrer's formula $S=K\lambda/\beta cos\theta$ [20-22]. Where K is constant equal to 0.9, λ is wavelength of CuKα radiation (1.5409 A^0), β is the full width at half maxima (FWHM) of XRD peaks. In the present work, the crystallite size of the doped $La_{0.7}Ca_{0.2}Sr_{0.1}MnO_3$ estimated from X-ray line broadening of the (002) peak (maximum intensity peak) is about 18 nm.

3.2 Electrical properties:

Resistivity measurements were performed in the temperature range 2K under 3, 5, 10 and 14 T fields using Quantum Design PPMS. Fig. 2 shows the temperature dependence of the resistivity of $La_{0.7}Ca_{0.2}Sr_{0.1}MnO_3$ pellets in different magnetic fields. The sample at zero field exhibit a broad metal-insulator transition around ~ 213 K [23]. When magnetic field is applied the transition temperature is shifted and finally attains the value of ~ 250 K at 14 T.

At metal-insulator transition temperature (T_{M-I}), $La_{0.7}Ca_{0.2}Sr_{0.1}MnO_3$ sample exhibit 13, 17, 28 and 35 % of negative MR for 3, 5, 10 and 14 T applied magnetic fields respectively. The variation of T_{M-I} against magnetic field is shown in Fig.3.

Fig. 4 shows magnetic field dependence of the resistivity of $La_{0.7}Ca_{0.2}Sr_{0.1}MnO_3$ sample measured at 150 K, 230 K and 300 K. At each temperature, the resistivity decreases with increase in magnetic field.

3.3Magnetotransport properties:

Fig. 5 shows magnetoresistance of the $La_{0.7}Ca_{0.2}Sr_{0.1}MnO_3$ sample in different temperature ranges. For low fields, there is a sharp decrease of MR. For high fields, a more gradual MR decrease is observed. Fig. 6 shows magnetic field dependent MR at temperature 150 K, 230 K and 300 K. It shows that MR value decreases as the temperature increases and at 300 K maximum value of MR is found to be ~ 22% for an applied field of 14

T. MR of ~ 28% is observed at 230 K. MR of ~ 35% is observed at 150 K in an applied field of 14 T and MR has negative sign.

IV. Figures

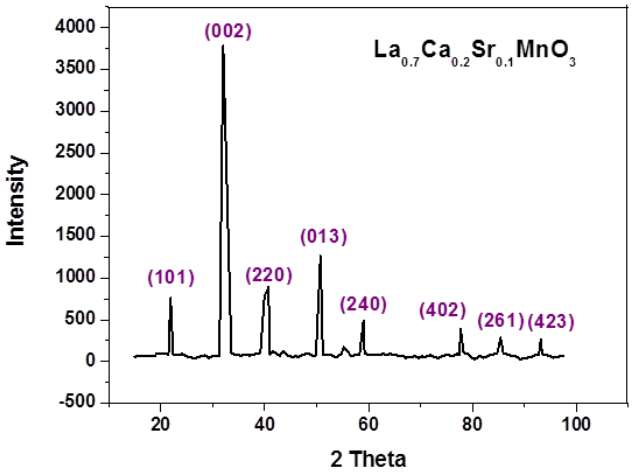

Fig. 1 XRD spectrum of $La_{0.7}Ca_{0.2}Sr_{0.1}MnO_3$.

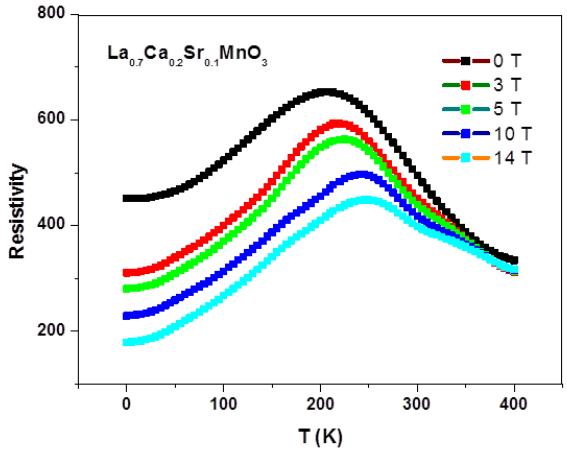

Fig.2 Temperature dependance of resistivity of $La_{0.7}Ca_{0.2}Sr_{0.1}MnO_3$ at various magnetic fields.

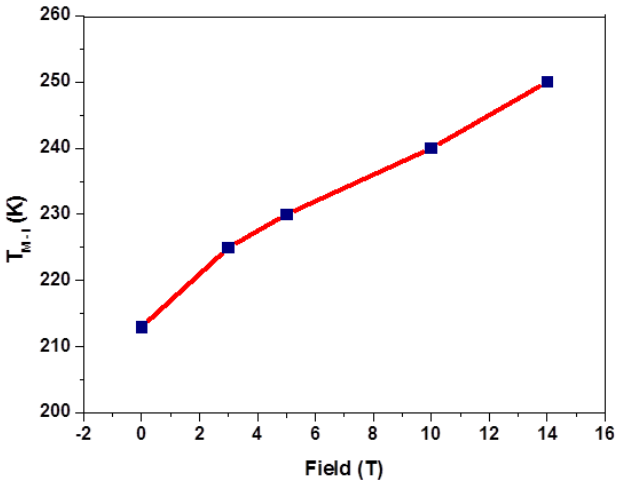

Fig. 3 Variation of Metal- Insulator temperature at various magnetic fields.

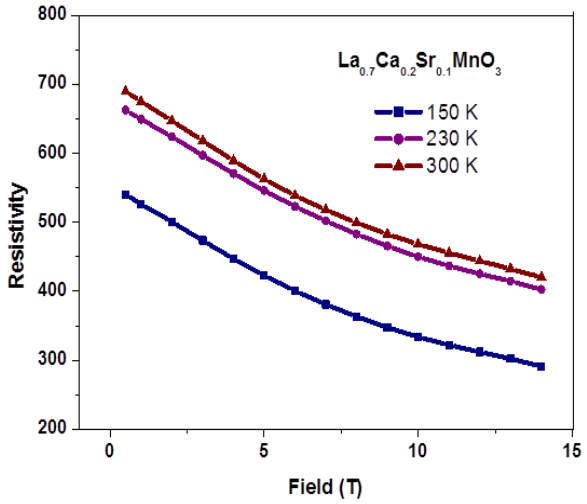

Fig. 4 Variation of resistivity of $La_{0.7}Ca_{0.2}Sr_{0.1}MnO_3$ with magnetic field.

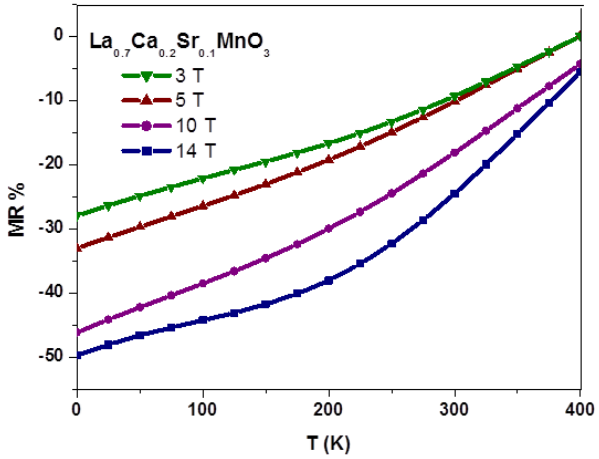

Fig. 5 Temperature variation of magnetoresistance of $La_{0.7}Ca_{0.2}Sr_{0.1}MnO_3$.

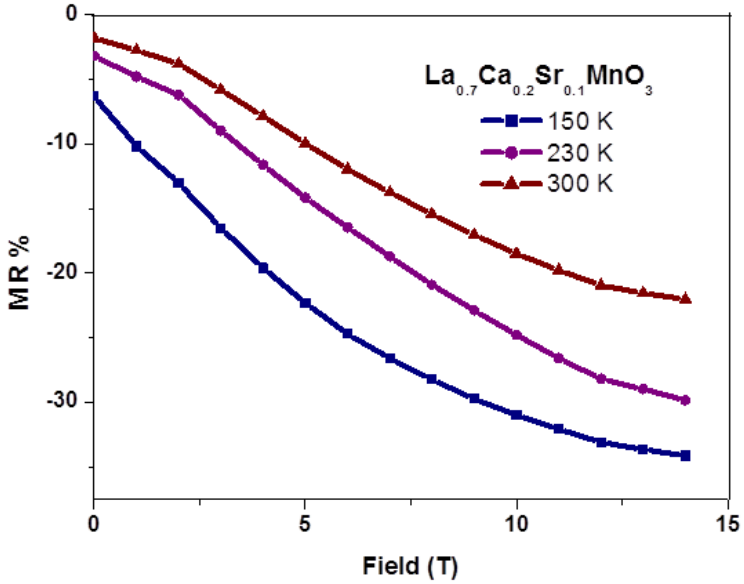

Fig. 6 Field dependence of MR% for $La_{0.7}Ca_{0.2}Sr_{0.1}MnO_3$ at different temperatures.

V. Conclusions

1. $La_{0.7}Ca_{0.2}Sr_{0.1}MnO_3$ samples were synthesized by solution combustion synthesis.
2. XRD spectrum of $La_{0.7}Ca_{0.2}Sr_{0.1}MnO_3$ reveals single phase nature. The diffraction peaks of $La_{0.7}Ca_{0.2}Sr_{0.1}MnO_3$ are sharp and crystallize in orthorhombic structure.
3. Crystallite sizes were estimated from the Scherrer's formula, and is calculated about 18 nm.
4. The temperature dependence resistivity of $La_{0.7}Ca_{0.2}Sr_{0.1}MnO_3$ pellets in different magnetic fields shows broad Metal–Insulator transition (T_{M-I}) At zero field, the sample exhibit a T_{M-I} around ~ 213 K and when the magnetic field is applied the transition temperature is shifted and finally attains the value of ~ 250 K at 14 T.
5. At metal-insulator transition temperature (T_{M-I}), $La_{0.7}Ca_{0.2}Sr_{0.1}MnO_3$ sample exhibit 13, 17, 28 and 35% of negative MR for 3, 5, 10 and 14 T applied magnetic fields respectively.

References

[1] G. W. Kim, M. S. Anwar, S. N. Heo, K. Y. Park and B. H. Koo, Tuning of Magnetoresistance in $(La_{0.67}Ca_{0.33}MnO_3)(0.97)/(ZnO)/(0.03)$ composite by modifaction of the sintering temperature, *J. Ceram. Proc. Res., 13*, 2012, 89-92.

[2] S. W. Han, J. D. Lee, K.H. Kim, H. Song, W.J. Kim, S.J. Kwon, H.G. Lee, J.I. Jeong and J.S. Kang, Electronic Structures of the CMR Perovskites $R_{1-x}A_xMnO_3$ (R = La, Pr; A = Ca, Sr, Ce) using Photoelectron Spectroscopy, *J. Kor. Phys. Soc. 40,* 2002, 501.

[3] S. Das and T.K. Dey, Electrical conductivity and low field magnetoresistance in polycrystalline La1KxKxMnO3 pellets prepared by pyrophoric method, *Solid State Commu., 134,* 2005, 837.

[4] K. Dorr, Ferromagnetic manganites: spin-polarized conduction versus competing interactions *J.Phys. D Appl. Phys. 39*, 2006, R125.

[5] H.Y. Hwang *et al*., Spin-Polarized Intergrain Tunneling in $La_{2/3}Sr_{1/3}MnO_3$, *Phys. Rev. Lett. 77,* 1996, 2041.

[6] A. Gaur and G.D. Verma, Electrical and magnetotransport properties of $La_{0.7}Sr_{0.3}MnO_3/TiO_2$ composites, *Crys. Res. Technol. 42(2)*, 2007, 164-168.

[7] M.B. Salamon, M. Jaime, The physics of manganites: Structure and transport, *Rev. Mod. Phys. 73,* 2001, 583.

[8] J.B. Goodenough, Theory of the Role of Covalence in the Perovskite-Type Manganites $[La,M(II)]MnO_3$, *Phys. Rev. Lett. 100*, 1955, 564.

[9] M. Mc Cormack, S. Jin, T.H. Tiefel, R.M. Fleming, and J.M. Phillips, Very large magnetoresistance in perovskite-like La-Ca-Mn-O thin films, *Appl. Phys. Lett. 64*, 1994, 22.

[10] C. Zener, Interaction between the *d*-shells in the transition metals, *Phys. Rev. 81,*1951, 440.

[11] J.H. Kuo, H.U. Anderson and D.M. Sparlin, Oxidation-reduction behavior of uundoped and Sr-doped $LaMnO_3$: Defect structure, electrical conductivity and thermoelectric power, *J. Solid State Chem. 87,* 1990, 55.

[12] C.N.R. Rao, A.K. Cheetham and R. Mahesh, Giant Magnetoresistance and related properties of rare-earth manganates and other oxide systems, *Chem. Mater. 8*, 1996, 2421-2432.

[13] H. Taguchi, D. Matsuda, M. Nagao, K. Tanihata, and Y. Miyamoto, Synthesis of Perovskite-Type $(La_{1-x}Sr_x)MnO_3$ (x= 0.3) at Low Temperature, *J. Am. Ceram. Soc. 75*, 1992, 201.

[14] M.S.G. Baythoun and F.R. Sale, Production of strontium-substituted lanthanum manganite perovskite powder by the amorphous citrate process, J. *Mater. Sci. 17,* 1982, 2757.

[15] S.T. Aruna *et al*., Combustion synthesis and properties of strontium substituted lanthanum manganites $La_{1-x}Sr_xMnO_3$ ($0 \leq x \leq 0.3$), *J. Mater. Chem. 7,* 1997, 2499.

[16] B. Ghosh, S. Kar, L.K. Brar, A.K. Raychaudhuri, Electronic transport in nanostructured films of $La_{0.67}Sr_{0.33}MnO_3$, *J. Appl. Phys. 98,* 2005, 094302.

[17] H.Y. Hwang, S.W. Cheong, N.P. Ong and B. Batlogg, Spin-Polarized Intergrain Tunneling in $La_{2/3}Sr_{1/3}MnO_3$, *Phys. Rev. Lett. 77*, 1996, 2041.

[18] S. Ekambaram, Combustion syntheis and characterization of new class of ZnO based ceramic pigments, *J. Alloys Compd. 390,* 2005, L4.

[19] M. Verelst et al., Metal-Insulator transitions in anion-excess$LaMnO_{3+\delta}$ controlled by the Mn^{4+} content, *J. Solid State Chem. 104,* 1993, 74.

[20] H. Klug, L. Alexander, X-ray Diffraction procedures, *John Wiley, New York*. 491, 1962.

[21] A. C. Bose, R. Ramamoorthy and S. Ramaswamy, Formability of Metastable Tetragonal Solid Solution in Nanocrystalline NiO-ZrO_2 Powder, *Mater. Lett. 44*, 2000, 203.

[22] A.A. Rabelo, M.C. de Macedo, D.M. de Aravyo melo, C.A. Pascocimos, A.E. Martinelli, R.M. de Nascimento, Synthesis and characterization of $La_{1-x}Sr_xMnO_{3\pm\delta}$ powders obtained by the polymeric precursor route, *Materials Research 14(1),* 2011, 91-96.

[23] R. Mahesh, R. Mahendiran, A. K. Raychaudhuri, C. N. R. Rao, Effect of particle size on the giant magnetoresistance of $La_{0.7}Ca_{0.3}MnO_3$, *Appl. Phys. Lett. 68,* 1996, 2291.